Acta Histochemica 124 (2022) 151952

Contents lists available at ScienceDirect

Acta Histochemica

journal homepage: www.elsevier.com/locate/acthis

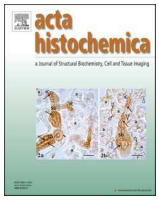

Optimizing immunostaining of archival fish samples to enhance museum collection potential

Garfield T. Kwan [a,c,*], Benjamin W. Frable [b], Andrew R. Thompson [c,1], Martin Tresguerres [a,1]

[a] Marine Biology Research Division, Scripps Institution of Oceanography, University of California San Diego, USA
[b] Marine Vertebrate Collection, Scripps Institution of Oceanography, University of California San Diego, USA
[c] NOAA Fisheries Service, Southwest Fisheries Science Center, La Jolla, CA, USA

ARTICLE INFO

Keywords:
Quenching
Antigen-retrieval
Formalin
Formaldehyde
Immunohistochemistry
Sodium borohydride

ABSTRACT

Immunohistochemistry (IHC) is a powerful biochemical technique that uses antibodies to specifically label and visualize proteins of interests within biological samples. However, fluid-preserved specimens within natural history collection often use fixatives and protocols that induce high background signal (autofluorescence), which hampers IHC as it produces low signal-to-noise ratio. Here, we explored techniques to reduce autofluorescence using sodium borohydride (SBH), citrate buffer, and their combination on fish tissue preserved with paraformaldehyde, formaldehyde, ethanol, and glutaraldehyde. We found SBH was the most effective quenching technique, and applied this pretreatment to the gill or skin of 10 different archival fishes – including specimens that had been preserved in formaldehyde or ethanol for up to 65 and 37 years, respectively. The enzyme Na^+/K^+-ATPase (NKA) was successfully immunostained and imaged using confocal fluorescence microscopy, allowing for the identification and characterization of NKA-rich ionocytes essential for fish ionic and acid-base homeostasis. Altogether, our SBH-based method facilitates the use of IHC on archival samples, and unlocks the historical record on fish biological responses to environmental factors (such as climate change) using specimens from natural history collections that were preserved decades to centuries ago.

1. Introduction

The potential of formaldehyde as a histological preservation agent was first recognized in the late 19th century (Simmons, 2014). By the early 20th century, formaldehyde was widely used in natural history collections to indefinitely preserve biological materials for morphological and taxonomic research (Simmons, 2014). Today, natural history collections contain an unparalleled array of biological specimens collected over the past centuries. As a result, natural history collections are often regarded as 'time machines' that allow researchers to examine and analyze samples collected decades to centuries ago (Shaffer et al., 1998). However, long-term formaldehyde preservation is known to denature DNA (Stollar and Grossman, 1962), alter δ13C and δ15N isotope signatures (Edwards et al., 2002; Kelly et al., 2006), and induce protein crosslinkage that impedes immunohistochemistry (IHC; Pikkarainen et al., 2010; Stradleigh and Ishida, 2015). Past and ongoing research are aimed at improving DNA extraction (reviewed in Card et al., 2021; Raxworthy and Smith, 2021) and isotopic analysis (Hetherington et al., 2019; reviewed in Sarakinos et al., 2002) from archival specimens, whereas this study focuses on optimizing IHC of archival fish samples to unlock information about protein abundance and localization.

IHC is a biochemical technique that uses antibody-antigen immunoreactivity to label proteins of interest. Although alcohol- or aldehyde-fixed tissues can be immunostained, tissues fixed with paraformaldehyde (PFA) is often preferable as it provides more optimal signal-to-noise ratio during imaging (Clancy and Cauller, 1998; Matsuda et al., 2011; Diez-Fraile et al., 2012). However, PFA is significantly more expensive than formaldehyde due to its extensive processing that is difficult to perform in field conditions (Simmons, 2014), and likely will not be widely adopted as the preservation agent across biological archives. Moreover, many of the fluid-preserved specimens within natural history collections around the world have been fixed with, or remain stored in formaldehyde. Thus, there is a great benefit to develop IHC

Abbreviations: SBH, sodium borohydride; IHC, immunohistochemistry; PFA, parafromaldehyde; GTA, glutaraldehyde; NKA, Na^+/K^+-ATPase.

* Corresponding author at: Marine Biology Research Division, Scripps Institution of Oceanography, University of California San Diego, USA.
E-mail address: gkwan09@gmail.com (G.T. Kwan).

[1] These authors contributed equally to this work.

https://doi.org/10.1016/j.acthis.2022.151952
Received 20 July 2022; Received in revised form 31 August 2022; Accepted 4 September 2022
Available online 10 September 2022

techniques applicable to formaldehyde-fixed samples curated within natural history collections.

Formaldehyde fixation adversely affects IHC by inducing excessive protein crosslinkage, which prevents proper antibody binding (c.f. Pikkarainen et al., 2010; Stradleigh and Ishida, 2015). Furthermore, formaldehyde fixation results in high levels of background signal, which masks the antibody-dependent signal and results in low signal-to-noise ratio (reviewed in Shi et al., 2011; Stradleigh and Ishida, 2015). One strategy often used to improve signal-to-noise ratio is by "quenching" background autofluorescence and endogenous peroxidase activity (reviewed in Shi et al., 1997, 2011). These quenching protocols are typically optimized for paraffin-embedded mammalian tissue sections using reagents such as sodium borohydride (SBH) or citrate buffer (CB) (Shi et al., 1993, 2011; Baschong et al., 2001; Luquin et al., 2010; Oliveira et al., 2010; Matsuda et al., 2011). In contrast, research dedicated to developing quenching protocols for formaldehyde-fixed, non-mammalian archival tissue has been scant. In fact, IHC studies attempting to revive archival fish tissue for whole-mount imaging has been virtually non-existent. Despite this lack of research, several studies have successfully used fluorescent IHC to immunotarget the enzyme Na^+-K^+-ATPase (NKA) in formaldehyde-fixed fish gill (Wilson et al., 2000; Kwan et al., 2019; Frommel et al., 2021), pseudobranch (Yang et al., 2014), and intestine (Esbaugh and Cutler, 2016). However, these successful immunostaining on formaldehyde-fixed samples required targeted dissection (only the tissue of interest was fixed), transfer of samples from fixatives to alcohol within hours (typically 8 – 24 h), quenching procedures, sectioning, and/or the use of confocal microscopy. Importantly, the targeted sampling and fixation duration sharply contrast with existing collection protocols: curators and collection managers are tasked with fixing an intact fish, which depending on its size, may take weeks to months for formaldehyde to permeate through the entire specimen. Furthermore, there may be limited reagents available during research collections, especially when at sea or remote field stations. As a result, the fixation duration of archival samples varies greatly, with some samples being preserved from weeks to years at a time. Given the immense amount of historical data chronicled within archival samples, it is necessary to test, develop, and validate a robust quenching protocol that is applicable to natural history collections.

Natural history collections also contain specimens fixed in other preservatives. Ethanol is arguably the oldest organic chemical used by humans, and it is known to have been used as a preservative as early as 1662 (Simmons, 2014). Because ethanol was relatively expensive and distorts specimens, its popularity as a fixative declined as the relatively cheaper formaldehyde became the dominant preservation agent in the 20th century. More recently, ethanol has renewed utilization since samples fixed in > 95% ethanol can preserve DNA (Card et al., 2021; Raxworthy and Smith, 2021) and do not dissolve $CaCO_3$ microstructures such as otoliths (Swalethorp et al., 2016). Next, glutaraldehyde (GTA) is another preservative sometimes used in museums that fixes tissue more effectively, but at a slower rate than formaldehyde. Thus, GTA is sometimes used in combination with formaldehyde to enhance strength and rate of fixation (Simmons, 2014; Stradleigh and Ishida, 2015), and their excellent preservation of cell ultrastructure facilitates scanning electron microscopy (SEM). Even though samples fixed with 95% ethanol or GTA are not intended for IHC (Kiernan, 2000; Matsuda et al., 2011), they may be viable alternatives if the background signal could be sufficiently dampened, and their immunoreactivity recovered.

This study aims to identify and validate a robust IHC technique on archived fish samples preserved with fixatives at durations that reflect those commonly found within natural history collections. In this study, wild-caught splitnose rockfish (*Sebastes diploproa*) gills were fixed in 4 % PFA, 3.7 % formaldehyde (10 % formalin), 7.4 % formaldehyde (20 % formalin), 95 % ethanol, and combined 3 % PFA, 0.35 % GTA in 0.1 M sodium cacodylate buffer (SEM fixative) at durations that reflect both experimental and archival sampling. Next, we tested the effectiveness of SBH, CB, or combined SBH and CB quenching on rockfish gills, and quantified their viability on reducing autofluorescence. Next, we validated the most promising of the three quenching treatments on archival samples housed at the *Scripps Institution of Oceanography (SIO) Marine Vertebrate Collection* (La Jolla, CA, USA) and the *CalCOFI Ichthyoplankton Collection* (La Jolla; La Jolla, CA, USA), some of which were preserved in formaldehyde and ethanol for as long as 65 and 37 years, respectively (Table 1). The *SIO Marine Vertebrate Collection* (SIO MVC) contains samples dating back to 1884, and houses ~2,000,000 fishes across ~5700 species (Singer et al., 2018; Frable, 2022). The majority of the SIO MVC samples are fixed in 3.7 % formaldehyde (10% formalin) diluted with DI-water and buffered with sodium tetraborate (3 g/L), and the rest of the SIO MVC samples are mainly preserved in 95 % ethanol. The *Ichthyoplankton Collection* at NOAA Southwest Fisheries Science Center (SWFSC) houses larval fish samples that have been consistently collected in the California Current Ecosystem by the California Cooperative Oceanic Fisheries Investigations (CalCOFI) since 1949, and includes ~75,000 larvae spanning across ~550 species (Moser et al., 2002). The majority of these specimens are fixed in 1.9 % formaldehyde (5 % formalin) diluted with seawater and buffered with sodium tetraborate (3 g/L). Roughly 3 months to 1 year later, the collected larval fish samples are sorted, then transferred to 1.1 % formaldehyde (3 % formalin) diluted with tap-water and buffered with sodium tetraborate (3 g/L). Ever since 1997, CalCOFI begun preserving samples from the port side of bongo nets in 95% ethanol (Thompson et al., 2017). Various PFA- and GTA-fixed specimens preserved for experimental analysis were provided by the Tresguerres lab (SIO) and other research groups to be used as a comparison with archival samples. Fish samples were immunostained against the enzyme NKA due to the many existing studies that have successfully imaged NKA-rich ionocytes within the skin (c.f. Varsamos et al., 2002a; Kwan et al., 2019) and gill (c.f. Christensen et al., 2012; Montgomery et al., 2022) of various teleost fishes, and its essential role in maintaining ionic and acid-base homeostasis (reviewed in Varsamos et al., 2005; Evans et al., 2005; Glover et al., 2013). Altogether, 10 fish species were whole-mount immunostained against NKA and visualized with fluorescent secondary antibodies on epifluorescence and confocal microscopy.

2. Methods

2.1. Tissue collection and fixation methods

Splitnose rockfish (*Sebastes diploproa*; N = 3) were collected via bottom trawl at 340 m depth off Coronado Island, San Diego, California, USA (trawl in: 32°40.88′N, 117° 23.5′W; trawl out: 32° 43.27′N, 117° 22.09′W) on May 12th, 2018. Rockfish gills were quickly extracted and preserved with one of five fixation methods: **1)** 4% PFA in phosphate buffer saline (PBS) at 4 °C for 8 h, transferred to 50 % ethanol at 4 °C for 12 h, then stored in 70% ethanol at 4 °C until processing, **2)** 3.7 % DI-diluted borate-buffered formaldehyde (commonly referred to as 10% buffered formalin) for 2 weeks, then stored in 50 % isopropyl alcohol at room temperature until processing, **3)** 7.4 % DI-diluted borate-buffered formaldehyde (commonly referred to as 20 % buffered formalin) for 2 weeks, then stored in 50 % isopropyl alcohol at room temperature until processing, **4)** 95 % ethanol at 4 °C for 8 h, then switched to fresh 95 % ethanol at room temperature until processing, or **5)** 3 % PFA, 0.35 % GTA in 0.1 M sodium cacodylate buffer at 4 °C for 8 h, transferred to 50 % ethanol at 4 °C for 12 h, then stored in 70 % ethanol at 4 °C until processing. Processing began ~3 months later on August 15th, 2018. For the sake of brevity, we will refer to the preservative "3 % PFA, 0.35 % GTA in 0.1 M sodium cacodylate buffer" simply as "*SEM fixative*".

2.2. Tissue embedding, sectioning, and epifluorescence imaging

Samples were processed following the protocol detailed in Kwan et al. (2020). Gill samples were dehydrated in ethanol (70%, 95%, 100%, 10 min each), incubated in SafeClear (three times; 10 min each),

Table 1
List of fishes tested, and relevant fixation information. PFA=paraformaldehyde. PBS=phosphate buffer saline. DI=deionized water. AKA=also known as. SW=seawater. FW=freshwater.

Species	Life Stage	Collector (s); *Source*	Year Sampled	Fixative employed	Fixing Duration	Storage Solution	Storage Duration
Splitnose Rockfish (*Sebastes diploproa*)	Adult	Ben Frable, Garfield Kwan; *SIO Student Cruise*	2018	Five different treatments; see methods for fixative, duration, and additional details.			
Bluefin Tuna (*Thunnus thynnus*)	Juvenile	Garfield Kwan, Martin Tresguerres; *Ichthus Unlimited*	2020	4 % PFA; diluted & buffered in PBS	12 h	70 % ethanol	2 years
Bocaccio (*Sebastes paucispinis*)	Adult	Carl Hubbs; *SIO Marine Vertebrate Collection,* SIO 51–264	1951	3.7 % formaldehyde; DI-diluted, borate-buffered (AKA *10 % formalin*)	~2 weeks	50 % isopropyl alcohol	71 years
Shortspine Combfish (*Zaniolepis frenata*)	Adult	Harold J Walker, Peter Franks; *SIO Marine Vertebrate Collection.* SIO 07–167	2007	3.7 % formaldehyde; DI-diluted, borate-buffered (AKA *10 % formalin*)	15 years	Same solution	n/a
Tilefish (*Malacanthus plumieri*)	Adult	Troy Baird; *SIO Marine Vertebrate Collection*, SIO 19–77	1985	95 % ethanol	37 years	Same solution	n/a
Splitnose Rockfish (*Sebastes diploproa*)	Juvenile	Phil Zerofski, Kaelan Prime, Garfield Kwan; *SIO Experimental Aquarium*	2019	3 % PFA, 0.35 GTA, 0.1 M sodium cacodylate buffer	8 h	70 % ethanol	3 years
Cowcod (*Sebastes levis*)	Larvae	Megan Human, Matt Craig, Garfield Kwan; *CalCOFI Ichthyoplankton Collection*	2020	4 % PFA; diluted & buffered in PBS	12 h	70 % ethanol	2 years
Yellowtail Kingfish (*Seriola lalandi*)	Larvae	Darren Parsons, Phil Munday, Alvin Setiawan; *Northland Marine Research Centre*	2017	4 % formaldehyde in phosphate buffer saline	20 months	70 % ethanol	3 years
Northern Anchovy (*Engraulis mordax*)	Larvae	CalCOFI Cruise PT5804; *CalCOFI Ichthyoplankton Collection*	1958	1.9 % formaldehyde; SW-diluted, borate-buffered (AKA *5 % formalin*)	3 months - 2 years	1.1 % formaldehyde; FW-diluted, borate-buffered (AKA *3 % formalin*)	63–65 years
Shortbelly Rockfish (*Sebastes jordani*)	Larvae	CalCOFI Cruise NH1202; *CalCOFI Ichthyoplankton Collection*	2012	95 % ethanol	10 years	Same solution	n/a
Yellowfin Tuna (*Thunnus albacares*)	Larvae	Jeanne Wexler; *Inter-American Tropical Tuna Commission, Achotines Laboratory*	2015	3 % PFA, 0.35 GTA, 0.1 M sodium cacodylate buffer	6 h	70 % ethanol	7 years

immersed in warm paraffin (65 °C; three times; 10 min each), then embedded in paraffin on an ice pack overnight. The next day, gill samples were sectioned using a microtome (12 μm thickness), mounted onto glass slides, dried overnight in an incubator (35 °C), and stored at room temperature.

On the day of imaging, paraffin was removed via SafeClear washes (three times; 10 min each), and rehydrated in a series of decreasing ethanol steps (100 %, 95 %, 70 %, 10 min each). Next, samples were subjected to one of the following four quenching methods: **1)** control (PBS), **2)** SBH (1.0 mg/ml) in ice cold PBS (six times; 10 min each), **3)** bath in heated CB (~95 °C for 15 min), or **4)** CB then SBH quenching procedure. Samples were then nuclear stained with Hoechst 33342 (5 μg/ml) at room temperature for 1 h, washed thrice with PBS with 0.1 % Tween (PBS-T), immersed in Fluoro-gel with Tris (Electron Microscopy Sciences; Hatfield, Pennsylvania, USA), mounted with a coverslip, and imaged on an epifluorescence microscope (Zeiss AxioObserver Z1; Oberkochen, Germany) equipped with filter cubes Zeiss 49 DAPI (excitation: 352 nm, emission: 455 nm), Zeiss 38 HE GFP (excitation: 493 nm, emission: 517 nm), and Zeiss 43 HE DsRed (excitation: 557 nm, emission: 572 nm) at 20x magnification (objective: Plan-Apochromat 20x/0.8 M27).

Immunostained images were captured using Zeiss Axiovision software at the same exposure duration (DAPI: 50 ms, GFP and DsRed: 1 s), and their brightness and contrast were not adjusted. Immunostained images were captured using Zeiss Axiovision software at the same exposure duration (DAPI: 50 ms, GFP and DsRed: 1 s), and their brightness and contrast were not adjusted. DAPI staining was excited at 335–383 nm, and detected at 420–470 nm. Fluorescence in the *green* channel was excited at 450–490 nm, and detected at 500–550 nm. Finally, fluorescence in the *red* channel was excited at 538–562 nm and detected at 570–640 nm.

2.3. Quantifying mean fluorescence intensity

Gill images were separated into green and red channels, converted to greyscale, then imported into FIJI (Schindelin et al., 2012). The fluorescence intensity of both gill filament and background signal were thrice measured (4 ×4 μm; 16 μm^2 per measurement) using the mean fluorescence intensity (MFI) quantification methods detailed in Shihan et al. (2021). To ensure sampling consistency, we sampled the gill filament and ensured no background space was present. Autofluorescence was calculated by subtracting gill filament signal from background signal (thrice measured, 4 ×4 μm; 16 μm^2 per measurement). MFI values are presented as a percentage by dividing from 255, the maximum value possible. In total, we examined three gill samples per combination of fixative and quenching method.

2.4. Validating IHC on archival samples

Whole-mount immunostaining using fluorescent secondary antibodies were detailed in Kwan and Tresguerres (2022), respectively. Comparison of quenching techniques across gill sections revealed SBH was the best treatment (see Results), and was selected as the method used to validate archival samples. In anticipation of higher background signal due to longer fixation period, the concentration and number of SBH washes were increased to 1.5 mg/ml and twelve times at 10 min each, respectively. Next, samples were washed with PBS-T at room temperature for 5 min, immersed in blocking buffer (PBS-T, 2% normal goat serum, 0.02 % keyhole limpet hemocyanin) at room temperature for 1 hr, then incubated with the primary antibodies (α5: 42 ng/ml in blocking buffer; Developmental Studies Hybridoma Bank, University of Iowa, Iowa City, USA) in blocking buffer at 4 °C overnight. The next day, samples were washed in PBS-T (three times; 10 min each), incubated with anti-mouse fluorescent secondary antibodies (Alexa Fluor 545;

1:1000), anti-rabbit fluorescent secondary antibodies (Alexa Fluor 488; 1:1000) and Hoechst 33342 (5 μg/ml; Invitrogen) at room temperature for 1 hr, washed in PBS-T (three times; 10 min each), then mounted onto depression slides with a cover slip.

AlexaFluor (to visualize NKA) was detected in archival samples using the Zeiss AxioObserver Z1 with a 20x objective (Plan-Apochromat 20x/0.8 M27). Samples were imaged for a total of four times: pre-SBH treatment (epifluorescence, DAPI, GFP, and DsRed: 100 ms), post-SBH treatment (epifluorescence, DAPI, GFP, and DsRed: 100 ms), post-immunostaining epifluorescence microscopy (epifluorescence, DAPI: 3 ms, GFP and DsRed: 40 ms), and post-immunostaining confocal microscopy (confocal, DAPI: 353 nm excitation at 0.8 % laser power, 465 nm emission, detection 410–470 nm; GFP: 493 nm excitation at 0.8 % laser power, 517 nm emission, detection 510–575 nm; DsRed: 577 nm excitation at 0.8 % laser power, 603 nm emission, detection 575–617 nm). Samples without primary antibodies (negative controls) revealed background fluorescence, but no specific ionocyte staining. Adult fishes were imaged on the trailing edge of the gill, whereas larval fishes were imaged on their skin immediately posterior to their respective operculum. Both post-immunostaining epifluorescence and confocal microscope images were Z-stacked imaged at the same location. Image brightness and contrast were not adjusted.

2.5. Statistical analysis

Statistical tests were performed using R (version 4.0.3; R Development Core Team, 2013). Shapiro-Wilks and Levene's test were used initially to test ANOVA's assumption of normality and homoscedasticity of variance. First, we ran Two-way ANOVA to evaluate the multiplicative effects of fluorescence channel and fixative on gill sections prior to quenching treatments. We followed this with Tukey's Honest Significant Difference (HSD) post-hoc to evaluate the significance of pairwise treatments. Second, we again used Two-way ANOVAs and Tukey HSDs tests to elucidate the effects of fixative and quenching. Because our first analysis (see Results) indicated differences between the green and red fluorescence, the two channels were evaluated as separate Two-way ANOVAs.

3. Result and discussion

3.1. Comparison of fixative-induced autofluorescence

Shapiro-Wilks and Levene's tests indicated that normality and variance assumptions were met for all comparisons. The interaction between fluorescence channel and fixative ($F_{4,20}$ =30.99, p = <0.0001) was significant among control, non-quenched samples (Two-way ANOVA; Supplemental Table 1). In addition, green MFI was significantly higher than red in all fixatives except 4 % PFA (Tukey HSD; Fig. 1). In the green channel, the autofluorescence of tissues fixed in 3.7 % formaldehyde, 7.4 % formaldehyde, and SEM fixative were significantly higher than those preserved with 4 % PFA (Fig. 1). However, the autofluorescence of tissues fixed in 95% ethanol was not significantly different from those preserved with 4 % PFA (Fig. 1). In contrast, the type of fixative did not affect autofluorescence in the red channel (Fig. 1). Altogether, these results suggest fixative-induced autofluorescence are channel/wavelength specific. Representative images of non-quenched rockfish gill tissues are shown in Figs. 2 and 3, respectively.

3.2. Impact of quenching on fixative-induced autofluorescence

Due to the disparity in green and red MFI within non-quenched samples, we conducted separate Two-way ANOVAS to analyze the effects of quenching on fixative-induced autofluorescence. For green autoflorescence, the interaction between fixative and quenching methods was highly significant (Two-way ANOVA; $F_{12,40}$ =22.83, p = <0.0001; Supplemental Table 2), and varied greatly from 9 % (4% PFA and SBH) to 91 % (SEM fixative and CB). In general, PFA-, 3.7 % and 7.4 % formaldehyde-, and SEM-fixed samples exhibited significantly reduced green autofluorescence following SBH quenching, and significantly greater green autofluorescence after CB or combined CB and SBH quenching (Fig. 2). The only exception was found in 4% PFA-fixed samples: SBH quenching reduced green autofluorescence by ~10% MFI (~50 % of control value), but statistical significance was not detected (Fig. 2). On the other hand, 95% ethanol-fixed samples were not affected by SBH and CB, but experienced greater green autofluorescence following combined SBH + CB incubation (Fig. 2).

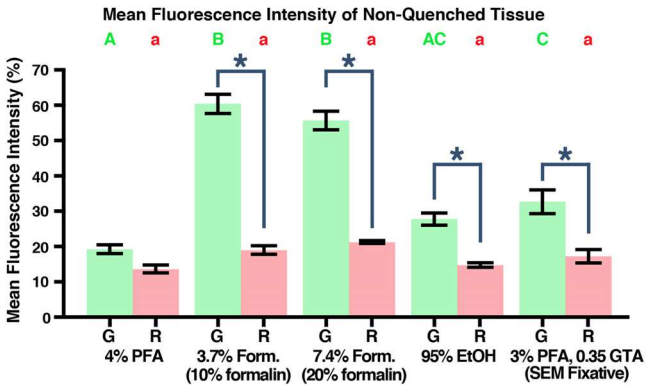

Fig. 1. Comparison of fixative-induced autofluorescence prior to quenching treatments in A) green and B) red channels. *Statistical analysis*: 2-way ANOVA with Tukey HSD. Results shown as mean ± SE. G=green, R=red, PFA=paraformaldehyde, Form.=formaldehyde, EtOH=ethanol, GTA=glutaraldehyde. Uppercased green letters denote significance among fixatives in the green fluorescence channels, and lowercased red letters denote significance among fixatives in the red fluorescence channels. Asterisk denote significance between fluorescence channels within fixative treatments.

For red autofluorescence, the interaction between fixative and quenching methods was also highly significant (Two-way ANOVA; $F_{12,40}$ =36.61, p = <0.0001; Supplemental Table 3) and varied from 2 % (4 % PFA and SBH) to 55 % (SEM fixative and CB). The direction in which red autofluorescence responds to the various quenching treatments was mostly consistent with those observed for green autofluorescence. Tukey's HSD indicated SBH quenching significantly reduced red autofluorescence in 4 % PFA-, 7.4 % formaldehyde-, and SEM-fixed samples, but did not significantly affect 3.7 % formaldehyde- and 95 % ethanol-fixed samples (Fig. 3). Next, CB quenching significantly increased red autofluorescence in 3.7 % and 7.4 % formaldehyde- and SEM-fixed samples, but did not significantly affect samples preserved with 4 % PFA and 95 % ethanol (Fig. 3). Finally, combined SBH and CB resulted in significantly higher red autofluorescence in 3.7 % formaldehyde-fixed samples, and did not significantly change samples preserved in 4 % PFA, 7.4 % formaldehyde, 95 % ethanol, or SEM fixative (Fig. 3).

In summary, SBH incubation generally reduced a considerable amount of red and green autofluorescence in PFA-, formaldehyde- and GTA-fixed samples. Because SBH is a known aldehydic reducing agent (Abdel-Akher et al., 1952), its capacity to reduce cross-linkage caused by aldehyde fixatives (i.e. PFA, formaldehyde, GTA) (Thavarajah et al., 2012) should not be surprising. Moreover, this may explain why samples preserved with 95 % ethanol failed to improve following SBH incubation since their observed autofluorescence was not derived from the aldehyde. Finally, quenching with CB alone or in combination with SBH barely reduced autofluorescence, indicating that high temperature and alkaline hydrolysis are not appropriate for reducing background signal in aldehyde- and ethanol-preserved archival fish samples.

3.3. Validating fluorescent IHC on whole-mount archival samples

Because SBH was the most effective at quenching autofluorescence on cross sections, we tested this treatment on whole-mount archival fish

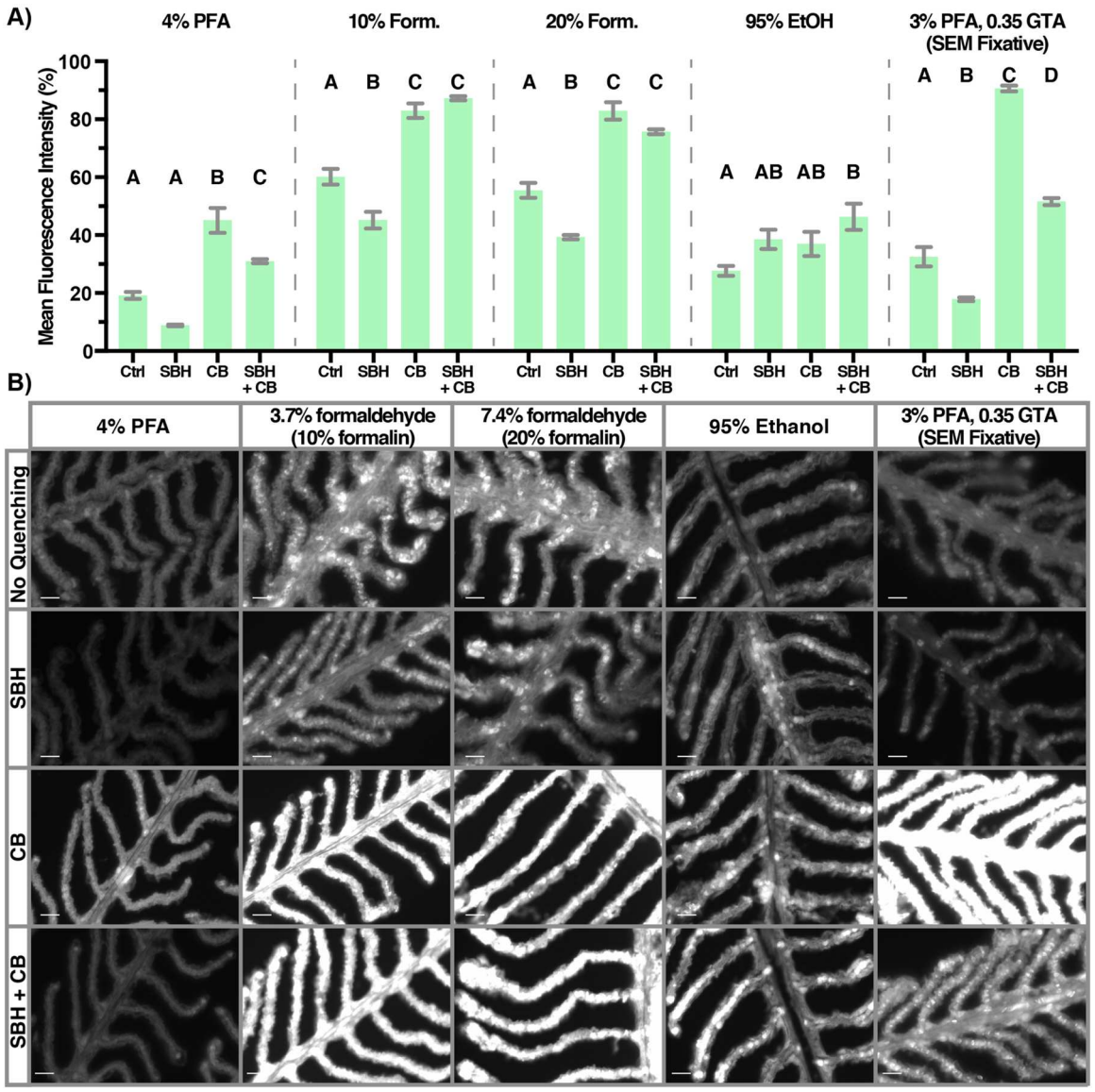

Fig. 2. A) Comparison of quenching treatments on fixative-specific autofluorescence in the green channel (excitation: 450–490 nm, detection: 500–550 nm), and B) representative image of gill autofluorescence. All images were captured using the same settings, and none of the images were altered. Alphabet letters denote significance among quenching treatment within fixative. *Statistical analysis*: Two-way ANOVA with Tukey HSD. Results shown as mean ± SE. Ctrl=control (no quenching), PFA=paraformaldehyde, GTA=glutaraldehyde, EtOH=ethanol, SBH=sodium borohydride, CB=citrate buffer. Scale bar= 20 μm.

samples to determine if it could help make IHC viable on natural history collections. To this aim, we selected archived fish samples from different species that had been fixed and preserved under various conditions and durations (Table 1). We chose NKA as the protein-of-interest because its presence and localization has been abundantly documented using IHC both in larval fish skin (reviewed in Varsamos et al., 2005) and adult fish gills (reviewed in Hwang and Lee, 2007; Hwang et al., 2011). Similar to our results in cross-sections, SBH incubation dramatically reduced autofluorescence in whole-mount samples fixed with PFA, formaldehyde, and GTA – but not in samples fixed with 95% ethanol (Supplemental Figs. 1, 2).

Next, we assessed whether we could visualize NKA within the skin and gill of various archival samples using epifluorescence microscopy (Fig. 4). As expected, NKA-rich ionocytes were most discernable in samples with low background signals such as the recently PFA-fixed bluefin tuna gill and cowcod skin (Fig. 4A,B). Additionally, the SBH treatment successfully increased the signal-to-noise ratio in formaldehyde-fixed yellowtail kingfish skin (fixed for 20 months) to levels comparable to the PFA-fixed samples (Fig. 4D). However, this improvement was not consistently observed across all formaldehyde-fixed samples. For instance, NKA signal in bocaccio gill and shortspine combfish gill (formaldehyde-fixed for 2 weeks and 15 years, respectively; Fig. 4C,E) were somewhat visible despite relatively high autofluorescence, whereas NKA signal was not detectable in Northern anchovy skin (formaldehyde fixed for 71 years) despite relatively low autofluorescence (Fig. 4F). This indicates that the duration of formaldehyde fixation affects the signal-to-noise ratio. The tilefish gill and shortbelly rockfish skin samples (Fig. 4G,H), which respectively had been fixed and stored in 95% ethanol for 37 and 10 years, had intensely bright autofluorescence that drowned out any NKA signal that may have been present. Conversely, despite relatively low autofluorescence, NKA signal was not observed in PFA+GTA-fixed splitnose rockfish gill and yellowfin tuna skin (Fig. 4I,J).

In an attempt to filter the NKA signal from the background and out-of-focus noise, we next tried confocal microscopy. This technique greatly enhanced signal-to-noise ratio and allowed us to identify NKA-rich ionocytes even in samples with high background tissue autofluorescence and dim NKA signal, regardless of fixative and fixation

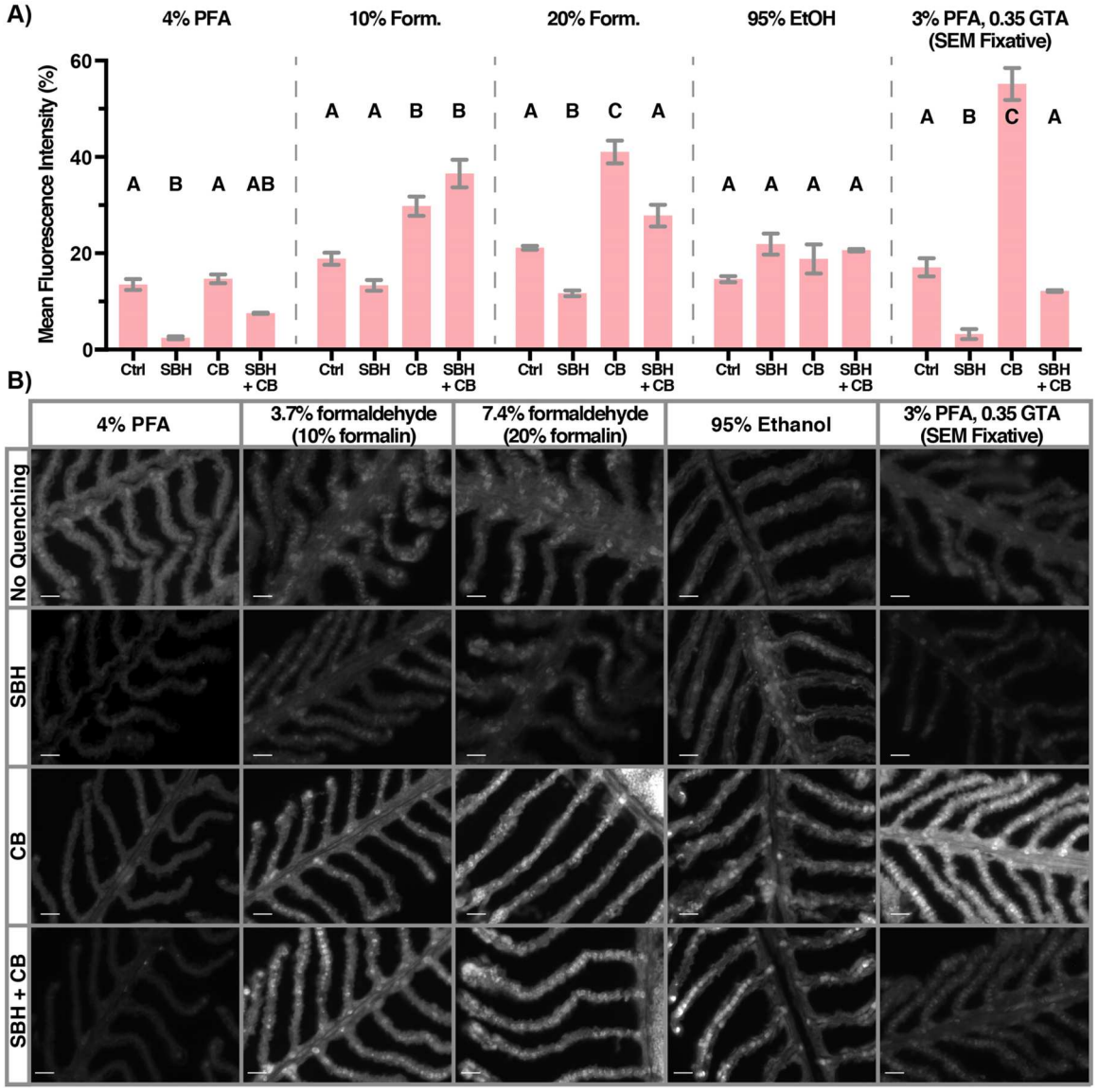

Fig. 3. A) Comparison of quenching treatments on fixative-specific autofluorescence in the red channel (excitation: 538–562 nm, detection: 570–640 nm), and B) representative image of gill autofluorescence. All images were captured using the same settings, and none of the images were altered. Alphabet letters denote significance among quenching treatment within fixative. *Statistical analysis*: Two-way ANOVA with Tukey HSD. Results shown as mean ± SE. Ctrl=control (no quenching), PFA=paraformaldehyde, GTA=glutaraldehyde, EtOH=ethanol, SBH = sodium borohydride, CB=citrate buffer. Scale bar= 20 μm.

duration (Fig. 5). In recently PFA-fixed bluefin tuna gill and cowcod skin, the NKA signal was very sharp (Fig. 5A,B) and greatly enhanced compared to that obtained using epifluorescence (compare to Fig. 4A,B). A sharp NKA signal was also observed in samples that were formaldehyde-fixed for relatively short periods (bocaccio gill, 2 weeks; yellowtail kingfish skin, 20 months) (Fig. 5 C,D), which was comparable to that of PFA-fixed samples. Confocal microscopy also greatly enhanced NKA signal in samples that were formaldehyde-fixed for longer durations (shortspine combfish gill, 15 years; Northern anchovy skin, 63–65 years) (Fig. 5 E,F), though their background signals remained apparent. In addition, confocal microscopy was able to distinguish the NKA signal in ethanol-fixed tilefish gill and Northern anchovy skin (albeit with high background signal; Fig. 5G,H) and in PFA+GTA-fixed splitnose rockfish gill and yellowfin tuna skin (Fig. 5I,J). These results demonstrate the combination of SBH quenching and confocal microscopy can be used to successfully immunolabel archival samples with fluorescent probes and produce images of higher quality compared to those captured using epifluorescence microscopy.

3.4. Implications for natural history collections

This study demonstrates the feasibility of using immunofluorescence microscopy on archival samples, including those that have been immersed in formaldehyde- or ethanol for multiple decades. We found repeated SBH washes greatly reduced autofluorescence in tissues preserved with aldehyde-based fixatives, and greatly enhanced downstream immunostaining and imaging. While epifluorescence imaging could not adequately detect our protein-of-interest in formaldehyde-, ethanol-, and GTA-fixed samples, confocal microscopy was able to resolve the NKA signal from the background in both red and green channels regardless of fixative and fixation duration. Altogether, this study suggests archival samples from natural history collections can be immunostained with relatively high success.

The duration of formaldehyde fixation ranges from weeks to years depending on specimen size, collection protocols, and resource constraints. Here, we demonstrated that formaldehyde-fixed samples that were transferred into isopropyl alcohol after ~2-weeks (bocaccio gill) and into ethanol after 2-years' time (yellowtail kingfish skin) can be

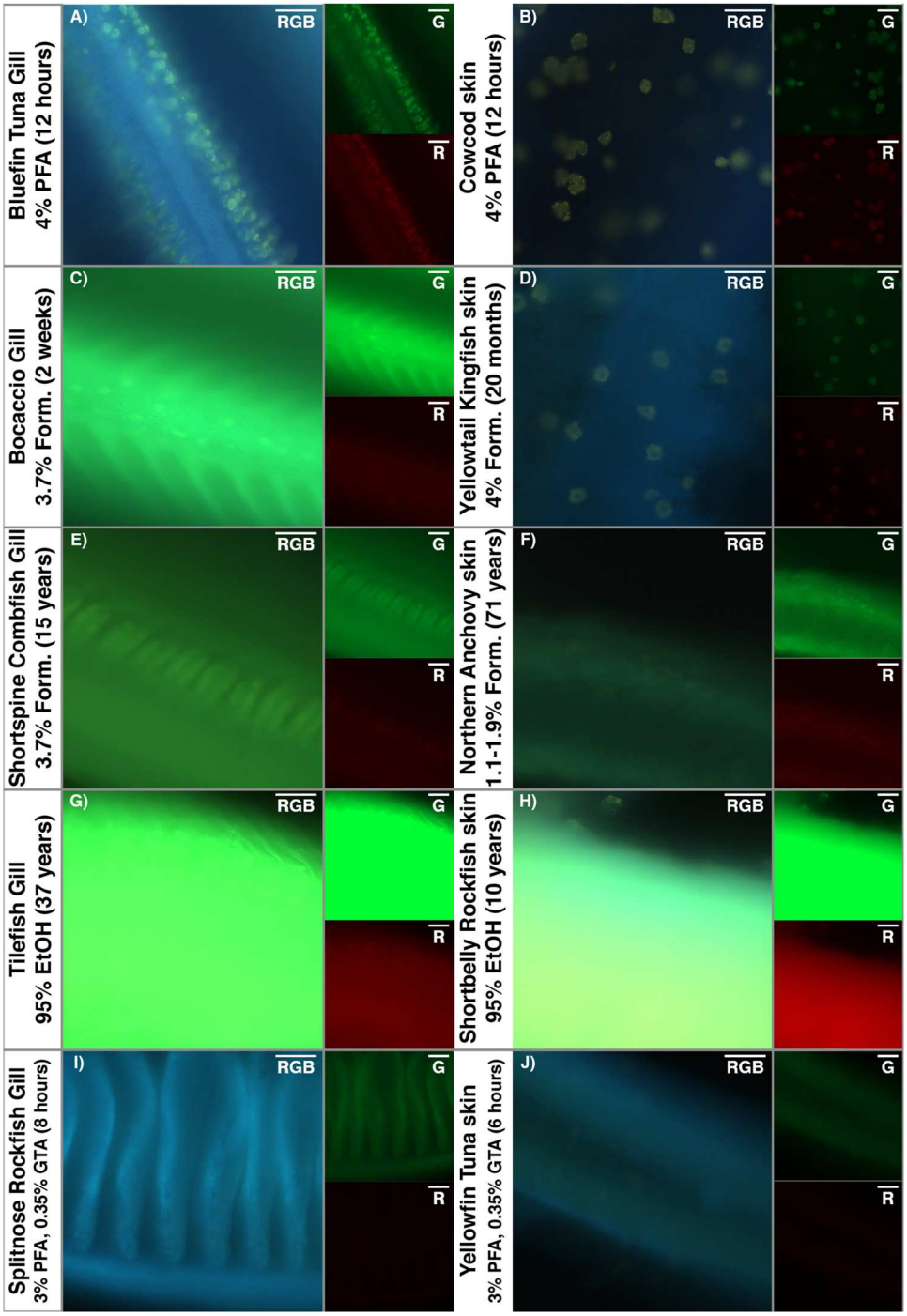

Fig. 4. NKA (green, red) within fish samples preserved with various fixatives and fixation duration were whole-mount imaged with epifluorescence microscopy. Images show a single image as high background signal prevents maximum intensity projection. Brightness and contrast were not adjusted. PFA=paraformaldehyde, Form.=formaldehyde, GTA=glutaraldehyde, EtOH=ethanol. Scale bar= 20 μm.

sufficiently quenched of autofluorescence to produce IHC at a quality that rival samples preserved with PFA (bluefin tuna gill, cowcod skin). In particular, the 2-week, 3.7% formaldehyde-fixed bocaccio sample had been stored in isopropyl alcohol for ~71 years, and the quality of the resulting IHC images are particularly encouraging as many archival samples are eventually transferred into alcohol for long-term storage once the specimen is thought to be properly preserved.

Natural history collections sometimes opt to keep specimens in formaldehyde to avoid the shrinkage effect associated with ethanol preservation. We observed extended formaldehyde fixation resulted in higher autofluorescence and obvious differences in IHC quality when compared to the formaldehyde-fixed specimens that were eventually transferred into alcohol (e.g. bocaccio and yellowtail kingfish). Even so, the signal-to-noise ratio was sufficiently high to identify the NKA signal in samples fixed in formaldehyde for 15 (shortspine combfish gill) and 65 years (Northern anchovy skin). Thus, specimens that have been completely formaldehyde-immersed for extended periods of time can still be viable for IHC. We believe this study is the first to successfully immunostained an archival fish specimen that was formaldehyde-preserved for 65 years.

Ethanol- and PFA+GTA-fixed samples were included to demonstrate their capacity as a last resort. Although SBH had little impact on the

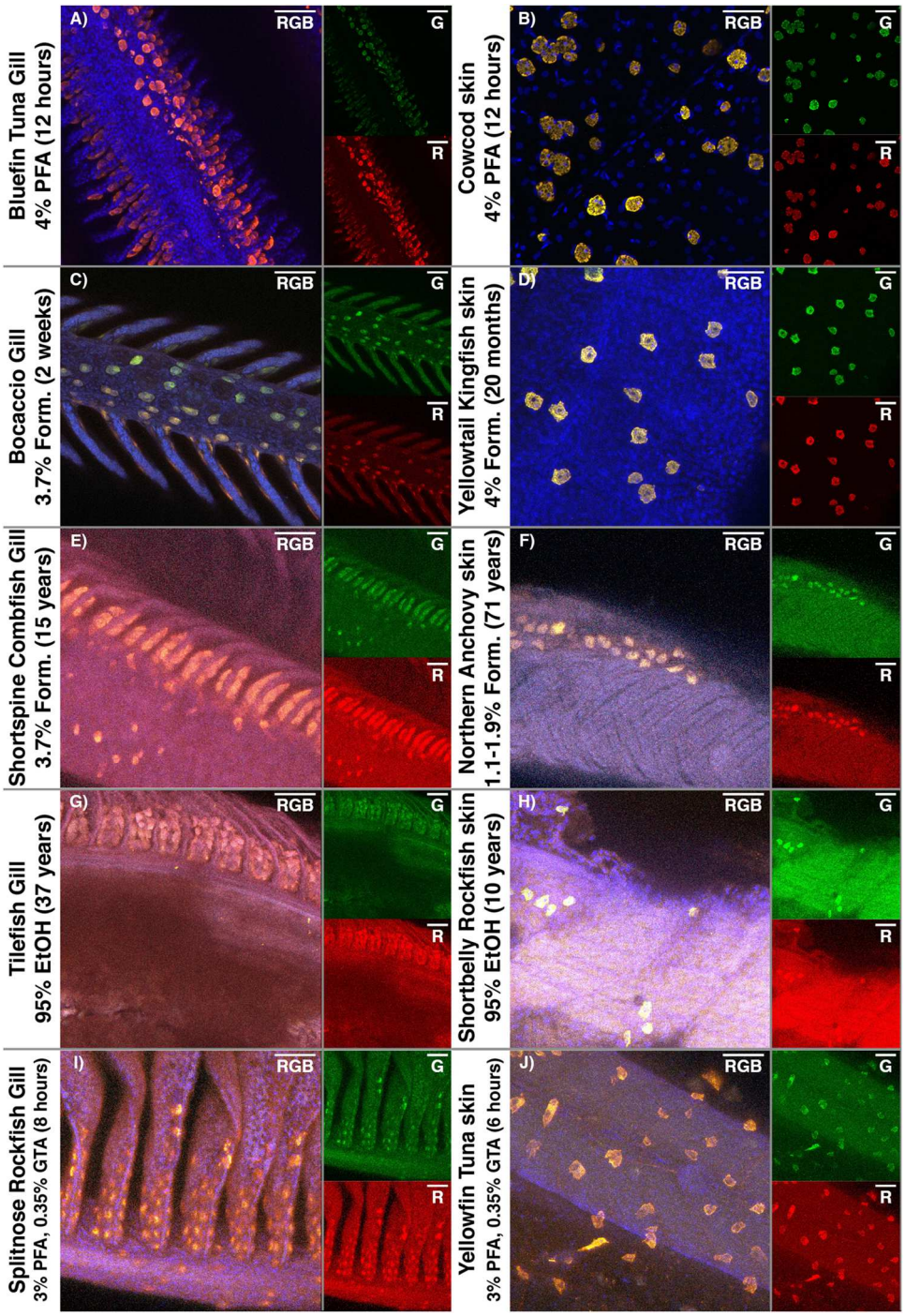

Fig. 5. NKA (green, red) in fish samples preserved with various fixatives and fixation duration were whole-mount imaged with confocal microscopy. Images are shown as maximum intensity projection. Brightness and contrast were not adjusted. PFA=paraformaldehyde, Form.=formaldehyde, GTA=glutaraldehyde, EtOH=ethanol. Scale bar= 20 μm.

autofluorescence of ethanol-fixed samples, confocal microscopy was still capable of immunostaining our protein-of-interest. In contrast, although SBH reduced autofluorescence in PFA+GTA-fixed samples, these still exhibited high background autofluorescence, and the resulting quality was similar to those fixed with ethanol- and formaldehyde-fixed specimens.

Due to the comparative nature of this study, we standardized imaging parameters including exposure duration, laser intensity, and channel-specific brightness and contrast levels. However, sample-specific adjustments would undoubtedly have enhanced the image quality of specimens fixed with non-optimal preservation methods; for example by fine-tuning laser settings and utilizing fluorophores that emit at wavelengths that do not overlap with tissue autofluorescence. In addition, confocal microscope software has the capacity to subtract specific wavelengths, which can also be used to reduce autofluorescence. On another note, SBH could be used to quench autofluorescence for other techniques such as fluorescent in situ hybridization (FISH), especially in ethanol-fixed, DNA/RNA stable specimens (Oliveira et al., 2010; Benerini Gatta et al., 2012).

By optimizing IHC on archival samples, we provide a valuable tool to examine biological responses across archives collected from decades to centuries ago. For instance, the NKA-rich ionocytes are ion-transporting

cells responsible for maintaining osmotic and acid-base homeostasis in fish (reviewed in Evans et al., 2005; Marshall and Grosell, 2006). As climate change progresses and aquatic habitats are modified due to anthropogenic activities, immunostained gill and skin NKA-rich ionocytes can be used as biomarkers of the physiological status of fish to establish baselines, monitor changes, and better predict physiological responses of fishes. For instance, the ion-transporting protein machinery within NKA-rich ionocytes changes according to environmental salinity (reviewed in Hiroi and McCormick, 2012), and the abundance of NKA-rich ionocytes may increase in response to hyper- (Varsamos et al., 2002b) and hypo-osmotic stress (Uchida and Kaneko, 1996; Sasai et al., 1998; Hirai et al., 1999; Zydlewski and McCormick, 2001). Today, rivers are increasingly diverted for use in farmlands, dams, and cities (e.g. San Francisco Estuary), and estuarine environments are becoming more saline due to saltwater intrusion (Cloern et al., 2011; Hutton et al., 2016). The SBH-quenching and IHC techniques described here can allow to identify potential changes in protein expression and ionocyte abundance by comparing archived estuarine fishes to contemporary specimens. Similarly, IHC on archived fish specimens can be applied to other aquatic habitats to assess the biological responses of climate change across decadal and centurial timescales.

The techniques described in this paper should also be applicable to other proteins and biological samples as long as adequate antibodies exist or are developed. These techniques could also be used for other fish organs that have already been immunostained with NKA and other antibodies including inner ear (Kwan and Tresguerres, 2022), intestine (Tresguerres et al., 2010), muscle, liver (Salmerón et al., 2021), and eye (Damsgaard et al., 2020). And since the basic principles of immunostaining and quenching are universal, these techniques should also be applicable to tissues from other organisms (e.g. annelids, arthropods, mollusks) archived within natural history collections. However, further optimization should be expected due to differences in fixation speed: the fixative requires more time to permeate through a larger sample and thus internal organs such as the intestine or muscles would take longer to get fixed compared to the skin and gills. Furthermore, external chitinous and calcium carbonate exoskeletons can also slow fixation and affect IHC. Therefore, further research is needed to optimize and validate IHC on other archived organs and organisms, which could use the SBH quenching and IHC techniques described here as a starting point. Other quenching strategies worth exploring include photobleaching with UV irradiation, ammonia + ethanol washes, and staining with Sudan Black B dye (Ramos-Vara, 2005; Oliveira et al., 2010; Allmon and Esbaugh, 2017). On another note, antigen-retrieval techniques should be explored in the event that background autofluorescence is dim yet IHC signal remains low. Antigen-retrieval techniques were mainly developed in formalin-fixed paraffin-embedded mammalian tissue sections, and some common techniques include a combination of temperature, salt additives (e.g. urea, lead thiocyanate), and acid-base changes (Shi et al., 1993, 2004, 2011).

In summary, this study showcases the potential for using SBH quenching coupled with confocal microscopy to immunostain and analyze both freshly collected and historical specimens thereby providing researchers with another tool to explore biological responses over time. These techniques also allow studying archived endangered and extinct species, overall elevating the inherent value of natural history collections.

CRediT authorship contribution statement

Garfield T. Kwan: Conceptualization, Data curation, Formal analysis, Funding acquisition, Investigation, Methodology, Validation, Visualization, Writing – original draft, Writing – review & editing. **Benjamin W. Frable:** Resources, Writing – review & editing. **Andrew R. Thompson:** Resources, Writing – review & editing. **Martin Tresguerres:** Conceptualization, Funding acquisition, Supervision, Writing – review & editing.

Acknowledgement

GTK was funded by the National Science Foundation (NSF) Graduate Research Fellowship Program and NSF Postdoctoral Research Fellowship in Biology (Award #1907334). This project was also supported by SIO discretionary fund awarded to MT. We thank Dr. Jennifer Taylor and the R/V Robert Gordon Sproul crew members for the opportunity to collect rockfish. We are indebted to the *SIO Marine Vertebrate Collection* and the *CalCOFI Ichthyoplankton Collection* for providing valuable archival specimens, and their respective curators and collection managers for maintaining the natural history collections. We are also grateful to many researchers who collected and contributed specimens for this study, including Dr. Phil Hastings, Harold J. Walker, William Watson, Sherri Charter, Dr. Carl Hubbs, Dr. Peter Franks, Dr. Alejandro Buentello and the Ichthus Unlimited team, Dr. Troy Baird, Kaelan Prime, Dr. Darren Parsons, Dr. Phil Munday, Dr. Alvin Setiawan, the Northland Marine Research Centre team, Megan Human, Dr. Matt Craig, Jeanne Wexler, the technical staff at Achotines Laboratory in Panama, Dr. Daniel Margulies, Vernon Scholey, the Inter-American Tropical Tuna Commission, the CalCOFI crew and scientists abroad the R/V Paolina T. on cruise 5804 and R/V New Horizon cruise 1202.

Appendix A. Supporting information

Supplementary data associated with this article can be found in the online version at doi:10.1016/j.acthis.2022.151952.

References

Abdel-Akher, M., Hamilton, T.K., Montgomery, R., Smith, F., 1952. A new procedure for the determination of the fine structure of polysaccharides. J. Am. Chem. Soc. 74, 4970–4971. https://doi.org/10.1021/ja01139a526.

Allmon, E.B., Esbaugh, A.J., 2017. Carbon dioxide induced plasticity of branchial acid-base pathways in an estuarine teleost. Sci. Rep. 7, 45680. https://doi.org/10.1038/srep45680.

Baschong, W., Suetterlin, R., Laeng, R.H., 2001. Control of autofluorescence of archival formaldehyde-fixed, paraffin-embedded tissue in confocal laser scanning microscopy (CLSM. J. Histochem. Cytochem. 49, 1565–1572. https://doi.org/10.1177/002215540104901210.

Benerini Gatta, L., Cadei, M., Balzarini, P., et al., 2012. Application of alternative fixatives to formalin in diagnostic pathology. Eur. J. Histochem. 56, 63–70. https://doi.org/10.4081/ejh.2012.e12.

Card, D.C., Shapiro, B., Giribet, G., et al., 2021. Museum genomics. Annu. Rev. Genet. 55, 633–659. https://doi.org/10.1146/annurev-genet-071719-020506.

Christensen, A.K., Hiroi, J., Schultz, E.T., McCormick, S.D., 2012. Branchial ionocyte organization and ion-transport protein expression in juvenile alewives acclimated to freshwater or seawater. J. Exp. Biol. 215, 642–652. https://doi.org/10.1242/jeb.063057.

Clancy, B., Cauller, L.J., 1998. Reduct. Backgr. autofluorescence Br. pdf, 83, pp. 97–102.

Cloern, J.E., Knowles, N., Brown, L.R., et al., 2011. Projected evolution of California's San Francisco bay-delta-river system in a century of climate change. PLoS One. https://doi.org/10.1371/journal.pone.0024465.

Damsgaard, C., Lauridsen, H., Harter, T.S., et al., 2020. A novel acidification mechanism for greatly enhanced oxygen supply to the fish retina. Elife 9, 1–20. https://doi.org/10.7554/eLife.58995.

Diez-Fraile, A., Van, N., DHerde K, J.C., 2012. Optimizing multiple immunostaining of neural tissue. Appl. Immunocytochem. 345–442.

Edwards, A., Melanie, S., Thomas, F., 2002. Short- and long-term effects of fixation and preservation on stable isotope values (δ13C, δ15N, δ34S) of fluid-preserved museum specimens. Copeia 4, 1106–1112, 10.1643/0045-8511(2002)002[1106:SALTEO]2.0.CO;2.

Esbaugh, A.J., Cutler, B., 2016. Intestinal Na+, K+, 2Cl-cotransporter 2 plays a crucial role in hyperosmotic transitions of a euryhaline teleost. Physiol. Rep. 4, 1–12. https://doi.org/10.14814/phy2.13028.

Evans, D.H., Piermarini, P.M., Choe, K.P., 2005. The multifunctional fish gill: dominant site of gas exchange, osmoregulation, acid-base regulation, and excretion of nitrogenous waste. Physiol. Rev. 85, 97–177. https://doi.org/10.1152/physrev.00050.2003.

Frable B.W. (2022) Personal Communication: About the Marine Vertebrate Collection. ⟨https://scripps.ucsd.edu/marine-vertebrate-collection/about-marine-vertebrate-collection⟩. Accessed 9 Jun 2022.

Frommel, A.Y., Kwan, G.T., Prime, K.J., et al., 2021. Changes in gill and air-breathing organ characteristics during the transition from water- to air-breathing in juvenile Arapaima gigas. J. Exp. Zool. Part A Ecol. Integr. Physiol. 2456. https://doi.org/10.1002/jez.2456.

Glover, C.N., Bucking, C., Wood, C.M., 2013. The skin of fish as a transport epithelium: a review. J. Comp. Physiol. B Biochem. Syst. Environ. Physiol. 183, 877–891. https://doi.org/10.1007/s00360-013-0761-4.
Hetherington, E.D., Kurle, C.M., Ohman, M.D., Popp, B.N., 2019. Effects of chemical preservation on bulk and amino acid isotope ratios of zooplankton, fish, and squid tissues. Rapid Commun. Mass Spectrom. 33, 935–945. https://doi.org/10.1002/rcm.8408.
Hirai, N., Tagawa, M., Kaneko, T., et al., 1999. Distributional changes in branchial chloride cells during freshwater adaptation in Japanese Sea Bass Lateolabrax japonicus. Zool. Sci. 16, 43–49. https://doi.org/10.2108/zsj.16.43.
Hiroi, J., McCormick, S.D., 2012. New insights into gill ionocyte and ion transporter function in euryhaline and diadromous fish. Respir. Physiol. Neurobiol. 184, 257–268. https://doi.org/10.1016/j.resp.2012.07.019.
Hutton, P.H., Rath, J.S., Chen, L., et al., 2016. Nine decades of salinity observations in the san francisco bay and delta: modeling and trend evaluations J. Water Resour. Plan. Manag. 142, 04015069.doi: 10.1061/(asce)wr.1943-5452.0000617.
Hwang, P.P., Lee, T.H., 2007. New insights into fish ion regulation and mitochondrion-rich cells. Comp. Biochem. Physiol. - A Mol. Integr. Physiol. 148, 479–497. https://doi.org/10.1016/j.cbpa.2007.06.416.
Hwang, P.-P., Lee, T.-H., Lin, L.-Y., 2011. Ion regulation in fish gills: recent progress in the cellular and molecular mechanisms. AJP Regul. Integr. Comp. Physiol. 301, R28–R47. https://doi.org/10.1152/ajpregu.00047.2011.
Kelly, B., Dempson, J.B., Power, M., 2006. The effects of preservation on fish tissue stable isotope signatures. J. Fish. Biol. 69, 1595–1611. https://doi.org/10.1111/j.1095-8649.2006.01226.x.
Kiernan, J.A., 2000. Formaldehyde, formalin, paraformaldehyde and glutaraldehyde: what they are and what they do. Micros. Today 8, 8–13. https://doi.org/10.1017/s1551929500057060.
Kwan, G.T., Tresguerres, M., 2022. Elucidating the acid-base mechanisms underlying otolith overgrowth in fish exposed to ocean acidification. Sci. Total Environ. 823, 153690 https://doi.org/10.1016/j.scitotenv.2022.153690.
Kwan, G.T., Wexler, J.B., Wegner, N.C., Tresguerres, M., 2019. Ontogenetic changes in cutaneous and branchial ionocytes and morphology in yellowfin tuna (Thunnus albacares) larvae. J. Comp. Physiol. B Biochem. Syst. Environ. Physiol. 189, 81–95. https://doi.org/10.1007/s00360-018-1187-9.
Kwan, G.T., Smith, T.R., Tresguerres, M., 2020. Immunological characterization of two types of ionocytes in the inner ear epithelium of Pacific Chub Mackerel (Scomber japonicus. J. Comp. Physiol. B 190, 419–431. https://doi.org/10.1007/s00360-020-01276-3.
Luquin, E., Pérez-Lorenzo, E., Aymerich, M.S., Mengual, E., 2010. Two-color fluorescence labeling in acrolein-fixed brain tissue. J. Histochem. Cytochem. 58, 359–368. https://doi.org/10.1369/jhc.2009.954495.
Marshall, W.S., Grosell, M., 2006. Ion transport, osmoregulation, and acid-base balance. In: Evans, D.H., Claiborne, J.B. (Eds.), The Physiology of Fishes, third ed. CRC Press, Boca Raton, pp. 177–230.
Matsuda, Y., Fujii, T., Suzuki, T., et al., 2011. Comparison of fixation methods for preservation of morphology, RNAs, and proteins from paraffin-embedded human cancer cell-implanted mouse models. J. Histochem Cytochem 59, 68–75. https://doi.org/10.1369/jhc.2010.957217.
Montgomery, D.W., Kwan, G.T., Davison, W.G., et al., 2022. Rapid blood acid–base regulation by European sea bass (Dicentrarchus labrax) in response to sudden exposure to high environmental CO_2. J. Exp. Biol. https://doi.org/10.1242/jeb.242735.
Moser H.G., Charter R.L., Smith P.E., et al. (2002) Distributional atlas of fish larvae and eggs from Manta (surface) samples collected on CalCOFI surveys from 1977 to 2000.
Oliveira, V.C., Carrara, R.C.V., Simoes, D.L.C., et al., 2010. Sudan Black B treatment reduces autofluorescence and improves resolution of in situhybridization specific fluorescent signals of brain sections. Histol. Histopathol. 25, 1017–1024. https://doi.org/10.14670/HH-25.1017.
Pikkarainen, M., Martikainen, P., Alafuzoff, I., 2010. The effect of prolonged fixation time on immunohistochemical staining of common neurodegenerative disease markers. J. Neuropathol. Exp. Neurol. 69, 40–52. https://doi.org/10.1097/NEN.0b013e3181c6c13d.
R Development Core Team (2013) R: A language and environment for statistical computing. R foundation for statistical computing.
Ramos-Vara, J.A., 2005. Technical aspects of immunohistochemistry. Vet. Pathol. 42, 405–426. https://doi.org/10.1354/vp.42-4-405.
Raxworthy, C.J., Smith, B.T., 2021. Mining museums for historical DNA: advances and challenges in museomics. Trends Ecol. Evol. 36, 1049–1060. https://doi.org/10.1016/j.tree.2021.07.009.
Salmerón, C., Harter, T.S., Kwan, G.T., et al., 2021. Molecular and biochemical characterization of the bicarbonate-sensing soluble adenylyl cyclase from a bony fish, the rainbow trout Oncorhynchus mykiss. Interface Focus 11, 20200026. https://doi.org/10.1098/rsfs.2020.0026.
Sarakinos, H.C., Johnson, M.L., Vander Zanden, M.J., 2002. A synthesis of tissue-preservation effects on carbon and nitrogen stable isotope signatures. Can. J. Zool. 80, 381–387. https://doi.org/10.1139/z02-007.
Sasai, S., Kaneko, T., Hasegawa, S., Tsukamoto, K., 1998. Morphological alteration in two types of gill chloride cells in Japanese eels (Anguilla japonica) during catadromous migration. Can. J. Zool. 76, 1480–1487. https://doi.org/10.1139/z98-072.
Schindelin, J., Arganda-Carreras, I., Frise, E., et al., 2012. Fiji: an open-source platform for biological-image analysis. Nat. Methods 9, 676–682. https://doi.org/10.1038/nmeth.2019.
Shaffer, H.B., Fisher, R.N., Davidson, C., 1998. The role of natural history collections in documenting species declines. Trends Ecol. Evol. 13, 27–30. https://doi.org/10.1016/S0169-5347(97)01177-4.
Shi, S., Cote, R.J., Taylor, C.R., 1997. Antigen retrieval immunohistochemistry: past, present, and future. J. Histochem. Cytochem. 45, 327–343.
Shi, S.R., Chaiwun, B., Young, L., et al., 1993. Antigen retrieval technique utilizing citrate buffer or urea solution for immunohistochemical demonstration of androgen receptor in formalin-fixed paraffin sections. J. Histochem. Cytochem. 41, 1599–1604. https://doi.org/10.1177/41.11.7691930.
Shi, S.R., Datar, R., Liu, C., et al., 2004. DNA extraction from archival formalin-fixed, paraffin-embedded tissues: Heat-induced retrieval in alkaline solution. Histochem. Cell Biol. 122, 211–218. https://doi.org/10.1007/s00418-004-0693-x.
Shi, S.R., Shi, Y., Taylor, C.R., 2011. Antigen retrieval immunohistochemistry: Review and future prospects in research and diagnosis over two decades. J. Histochem. Cytochem. 59, 13–32. https://doi.org/10.1369/jhc.2010.957191.
Shihan, M.H., Novo, S.G., Le Marchand, S.J., et al., 2021. A simple method for quantitating confocal fluorescent images. Biochem. Biophys. Rep. 25, 100916 https://doi.org/10.1016/j.bbrep.2021.100916.
Simmons J.E. (2014) Fluid Preservation. Rowman & Littlefield, Plymouth, United Kingdom.
Singer, R.A., Love, K.J., Page, L.M., 2018. A survey of digitized data from u.S. Fish collections in the idigbio data aggregator. PLoS One 13, 1–20. https://doi.org/10.1371/journal.pone.0207636.
Stollar, D., Grossman, L., 1962. The reaction of formaldehyde with denatured DNA: spectrophotometric, immunologic, and enzymic studies. J. Mol. Biol. 4, 31–38. https://doi.org/10.1016/S0022-2836(62)80114-4.
Stradleigh, T.W., Ishida, A.T., 2015. Fixation strategies for retinal immunohistochemistry. Prog. Retin. Eye Res. 48, 181–202. https://doi.org/10.1016/j.preteyeres.2015.04.001.
Swalethorp, R., Nielsen, T.G., Thompson, A.R., et al., 2016. Early life of an inshore population of West Greenlandic cod Gadus morhua: spatial and temporal aspects of growth and survival. Mar. Ecol. Prog. Ser. 555, 185–202. https://doi.org/10.3354/meps11816.
Thavarajah, R., Mudimbaimannar, V.K., Elizabeth, J., et al., 2012. Chemical and physical basics of routine formaldehyde fixation. J. Oral. Maxillofac. Pathol. 16, 400–405. https://doi.org/10.4103/0973-029X.102496.
Thompson, A.R., Chen, D.C., Guo, L.W., et al., 2017. Larval abundances of rockfishes that were historically targeted by fishing increased over 16 years in association with a large marine protected area. R. Soc. Open Sci. https://doi.org/10.1098/rsos.170639.
Tresguerres, M., Levin, L.R., Buck, J., Grosell, M., 2010. Modulation of NaCl absorption by [HCO3-] in the marine teleost intestine is mediated by soluble adenylyl cyclase. AJP Regul. Integr. Comp. Physiol. 299, R62–R71. https://doi.org/10.1152/ajpregu.00761.2009.
Uchida, K., Kaneko, T., 1996. Enhanced chloride cell turnover in the gills of Chum Salmon fry in seawater. Zool. Sci. 13, 655–660. https://doi.org/10.2108/zsj.13.655.
Varsamos, S., Diaz, J., Charmantier, G., et al., 2002a. Location and morphology of chloride cells during the post-embryonic development of the European sea bass, Dicentrarchus labrax. Anat. Embryol. 205, 203–213. https://doi.org/10.1007/s00429-002-0231-3.
Varsamos, S., Diaz, J.P., Charmantier, G.U.Y., et al., 2002b. Branchial chloride cells in sea bass (Dicentrarchus labrax) adapted to fresh water, seawater, and doubly concentrated seawater. J. Exp. Zool. 293, 12–26. https://doi.org/10.1002/jez.10099.
Varsamos, S., Nebel, C., Charmantier, G., 2005. Ontogeny of osmoregulation in postembryonic fish: a review. Comp. Biochem Physiol. - A Mol. Integr. Physiol. 141, 401–429. https://doi.org/10.1016/j.cbpb.2005.01.013.
Wilson, J.M., Randall, D.J., Donowitz, M., et al., 2000. Immunolocalization of ion-transport proteins to branchial epithelium mitochondria-rich cells in the mudskipper (Periophthalmodon schlosseri). J. Exp. Biol. 203, 2297–2310.
Yang, S.H., Kang, C.K., Kung, H.N., Lee, T.H., 2014. The lamellae-free-type pseudobranch of the euryhaline milkfish (Chanos chanos) is a Na+, K+-ATPase-abundant organ involved in hypoosmoregulation. Comp. Biochem. Physiol. - A Mol. Integr. Physiol. 170, 15–25. https://doi.org/10.1016/j.cbpa.2013.12.018.
Zydlewski, J., McCormick, S.D., 2001. Developmental and environmental regulation of chloride cells in young American shad, Alosa sapidissima. J. Exp. Zool. 290, 73–87.

Supplemental Material

Supplemental Table 1: Relevant Tukey's HSD statistical details on green autofluorescence ~ fixative*quenching. α=0.05.

Pairwise Comparison	Mean Difference	Lower Hinge	Upper Hinge	Adjusted P Value	Significant?
7.4%f:Green-3.7%f:Green	-4.6849673	-14.29998	4.9300458	0.769763	No
4%pfa:Green-3.7%f:Green	-40.979521	-50.594534	-31.364508	0	Yes
95%EtOH:Green-3.7%f:Green	-32.468453	-42.083466	-22.85344	0	Yes
EMS:Green-3.7%f:Green	-27.59573	-37.210743	-17.980717	0.0000001	Yes
EMS:Green-95%EtOH:Green	4.8727233	-4.74229	14.4877365	0.731247	No
95%EtOH:Green-4%pfa:Green	8.5110675	-1.103946	18.1260807	0.1107787	No
EMS:Green-4%pfa:Green	13.3837909	3.768778	22.998804	0.0025509	Yes
4%pfa:Green-7.4%f:Green	-36.294553	-45.909567	-26.67954	0	Yes
95%EtOH:Green-7.4%f:Green	-27.783486	-37.398499	-18.168473	0.0000001	Yes
EMS:Green-7.4%f:Green	-22.910763	-32.525776	-13.295749	0.0000019	Yes
7.4%f:Red-3.7%f:Red	2.262963	-7.35205	11.8779761	0.9969485	No
4%pfa:Red-3.7%f:Red	-5.3539869	-14.969	4.2610262	0.6256692	No
95%EtOH:Red-3.7%f:Red	-4.232244	-13.847257	5.3827691	0.8522834	No
EMS:Red-3.7%f:Red	-1.7864488	-11.401462	7.8285643	0.9995053	No
4%pfa:Red-7.4%f:Red	-7.6169499	-17.231963	1.9980633	0.1997706	No
95%EtOH:Red-7.4%f:Red	-6.495207	-16.11022	3.1198062	0.3792554	No
EMS:Red-7.4%f:Red	-4.0494118	-13.664425	5.5656014	0.8804908	No
95%EtOH:Red-4%pfa:Red	1.1217429	-8.49327	10.7367561	0.9999896	No
EMS:Red-4%pfa:Red	3.5675381	-6.047475	13.1825513	0.9387269	No
EMS:Red-95%EtOH:Red	2.4457952	-7.169218	12.0608084	0.9946261	No
EMS:Red-EMS:Green	-15.463486	-25.078499	-5.8484727	0.0004805	Yes
95%EtOH:Red-95%EtOH:Green	-13.036558	-22.651571	-3.4215446	0.0033762	Yes
7.4%f:Red-7.4%f:Green	-34.324837	-43.93985	-24.709824	0	Yes
3.7%f:Red-3.7%f:Green	-41.272767	-50.88778	-31.657754	0	Yes
4%pfa:Red-4%pfa:Green	-5.6472331	-15.262246	3.96778	0.5595127	No

Supplemental Table 2: Relevant Tukey's HSD statistical details on green autofluorescence ~ fixative*quenching. α=0.05.

Pairwise Comparison	Mean Difference	Lower Hinge	Upper Hinge	Adjusted P Value	Significant?
4%pfa:CB+SBH-4%pfa:CB	-14.123007	-27.576062	-0.669951	0.0308279	Yes
4%pfa:Ctrl-4%pfa:CB	-25.944967	-39.398023	-12.491912	0.0000012	Yes
4%pfa:SBH-4%pfa:CB	-36.268105	-49.72116	-22.815049	0	Yes
4%pfa:Ctrl-4%pfa:CB+SBH	-11.821961	-25.275016	1.6310948	0.1459944	No
4%pfa:SBH-4%pfa:CB+SBH	-22.145098	-35.598154	-8.6920425	0.0000359	Yes
4%pfa:SBH-4%pfa:Ctrl	-10.323137	-23.776193	3.1299183	0.329417	No
3.7%f:CB+SBH-3.7%f:CB	4.25424837	-9.1988072	17.7073039	0.9994179	No
3.7%f:Ctrl-3.7%f:CB	-22.837124	-36.29018	-9.3840686	0.0000194	Yes
3.7%f:SBH-3.7%f:CB	-37.804444	-51.2575	-24.351389	0	Yes
3.7%f:Ctrl-3.7%f:CB+SBH	-27.091373	-40.544428	-13.638317	0.0000004	Yes
3.7%f:SBH-3.7%f:CB+SBH	-42.058693	-55.511748	-28.605637	0	Yes
3.7%f:SBH-3.7%f:Ctrl	-14.96732	-28.420376	-1.5142647	0.0162849	Yes
7.4%f:CB+SBH-7.4%f:CB	-7.1879739	-20.641029	6.2650817	0.8734535	No
7.4%f:Ctrl-7.4%f:CB	-27.435556	-40.888611	-13.9825	0.0000003	Yes
7.4%f:SBH-7.4%f:CB	-43.62841	-57.081465	-30.175354	0	Yes
7.4%f:Ctrl-7.4%f:CB+SBH	-20.247582	-33.700637	-6.7945261	0.0001931	Yes
7.4%f:SBH-7.4%f:CB+SBH	-36.440436	-49.893491	-22.98738	0	Yes
7.4%f:SBH-7.4%f:Ctrl	-16.192854	-29.64591	-2.7397985	0.0061561	Yes
95%EtOH:CB+SBH-95%EtOH:CB	9.34501089	-4.1080447	22.7980664	0.5008772	No
95%EtOH:Ctrl-95%EtOH:CB	-9.295817	-22.748873	4.1572386	0.5102015	No
95%EtOH:SBH-95%EtOH:CB	1.57494554	-11.87811	15.0280011	1	No
95%EtOH:Ctrl-95%EtOH:CB+SBH	-18.640828	-32.093883	-5.1877723	0.0007856	Yes
95%EtOH:SBH-95%EtOH:CB+SBH	-7.7700654	-21.223121	5.6829902	0.7908445	No
95%EtOH:SBH-95%EtOH:Ctrl	10.8707625	-2.582293	24.3238181	0.2501752	No
EMS:CB+SBH-EMS:CB	-39.000087	-52.453143	-25.547032	0	Yes
EMS:Ctrl-EMS:CB	-58.055425	-71.50848	-44.602369	0	Yes
EMS:SBH-EMS:CB	-72.748192	-86.201247	-59.295136	0	Yes
EMS:Ctrl-EMS:CB+SBH	-19.055338	-32.508393	-5.6022821	0.0005486	Yes
EMS:SBH-EMS:CB+SBH	-33.748105	-47.20116	-20.295049	0	Yes
EMS:SBH-EMS:Ctrl	-14.692767	-28.145822	-1.2397113	0.0201049	Yes

Supplemental Table 3: Relevant Tukey's HSD statistical details on red autofluorescence ~ fixative*quenching. α=0.05.

Pairwise Comparison	Mean Difference	Lower Hinge	Upper Hinge	Adjusted P Value	Significant?
4%pfa:CB+SBH-4%pfa:CB	-7.1691503	-16.31833	1.98002953	0.2961427	No
4%pfa:Ctrl-4%pfa:CB	-1.1801743	-10.329354	7.96900556	1	No
4%pfa:SBH-4%pfa:CB	-12.260915	-21.410095	-3.1117352	0.0013291	Yes
4%pfa:Ctrl-4%pfa:CB+SBH	5.98897603	-3.1602038	15.1381559	0.6042016	No
4%pfa:SBH-4%pfa:CB+SBH	-5.0917647	-14.240945	4.05741515	0.8336959	No
4%pfa:SBH-4%pfa:Ctrl	-11.080741	-20.229921	-1.9315609	0.0056729	Yes
3.7%f:CB+SBH-3.7%f:CB	6.78867102	-2.3605088	15.9378509	0.3854476	Yes
3.7%f:Ctrl-3.7%f:CB	-10.891721	-20.040901	-1.7425413	0.0071086	Yes
3.7%f:SBH-3.7%f:CB	-16.420741	-25.569921	-7.2715609	0.000006	Yes
3.7%f:Ctrl-3.7%f:CB+SBH	-17.680392	-26.829572	-8.5312123	0.0000012	Yes
3.7%f:SBH-3.7%f:CB+SBH	-23.209412	-32.358592	-14.060232	0	Yes
3.7%f:SBH-3.7%f:Ctrl	-5.5290196	-14.6782	3.62016025	0.7302007	No
7.4%f:CB+SBH-7.4%f:CB	-13.19207	-22.34125	-4.0428899	0.0004071	Yes
7.4%f:Ctrl-7.4%f:CB	-19.887582	-29.036762	-10.738402	0.0000001	Yes
7.4%f:SBH-7.4%f:CB	-29.337255	-38.486435	-20.188075	0	Yes
7.4%f:Ctrl-7.4%f:CB+SBH	-6.695512	-15.844692	2.45366787	0.4092248	No
7.4%f:SBH-7.4%f:CB+SBH	-16.145185	-25.294365	-6.9960053	0.0000086	Yes
7.4%f:SBH-7.4%f:Ctrl	-9.4496732	-18.598853	-0.3004934	0.0364347	Yes
95%EtOH:CB+SBH-95%EtOH:CB	1.83389978	-7.3152801	10.9830796	0.9999993	No
95%EtOH:Ctrl-95%EtOH:CB	-4.1815686	-13.330749	4.96761122	0.9638366	No
95%EtOH:SBH-95%EtOH:CB	3.0908061	-6.0583738	12.239986	0.9986403	No
95%EtOH:Ctrl-95%EtOH:CB+SBH	-6.0154684	-15.164648	3.13371144	0.5967071	No
95%EtOH:SBH-95%EtOH:CB+SBH	1.25690632	-7.8922735	10.4060862	1	No
95%EtOH:SBH-95%EtOH:Ctrl	7.27237473	-1.8768051	16.4215546	0.2743122	No
EMS:CB+SBH-EMS:CB	-42.988976	-52.138156	-33.839796	0	Yes
EMS:Ctrl-EMS:CB	-38.079434	-47.228613	-28.930254	0	Yes
EMS:SBH-EMS:CB	-51.946318	-61.095498	-42.797138	0	Yes
EMS:Ctrl-EMS:CB+SBH	4.90954248	-4.2396374	14.0587223	0.8696027	No
EMS:SBH-EMS:CB+SBH	-8.957342	-18.106522	0.19183781	0.0608723	No
EMS:SBH-EMS:Ctrl	-13.866885	-23.016064	-4.7177047	0.0001703	Yes

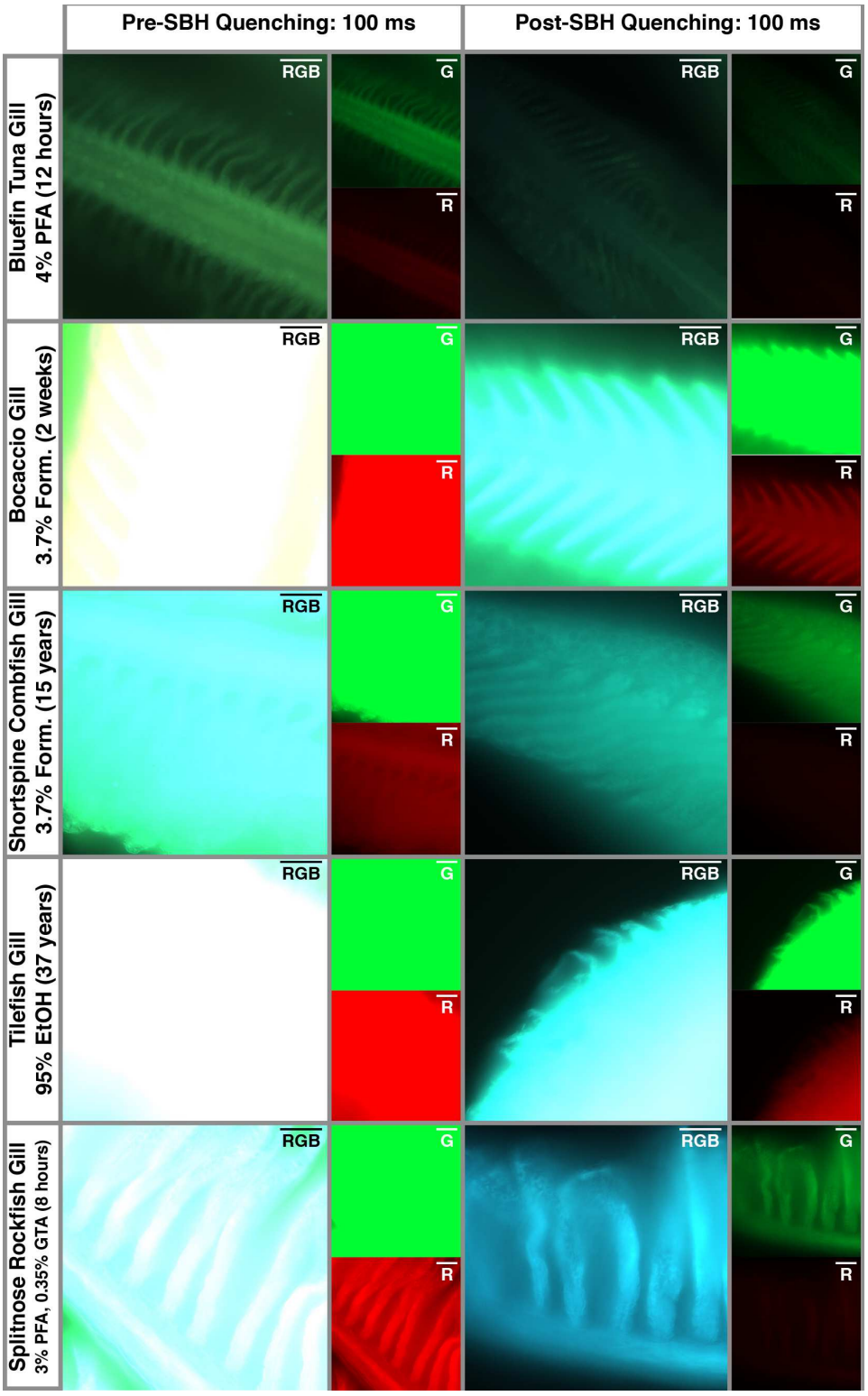

Supplemental Figure 1: Whole-mount epifluorescence images of various archival fish gills before and after sodium borohydride (SBH) quenching. PFA=paraformaldehyde, GTA=glutaraldehyde, EtOH=ethanol. Scale bar=20 μm.

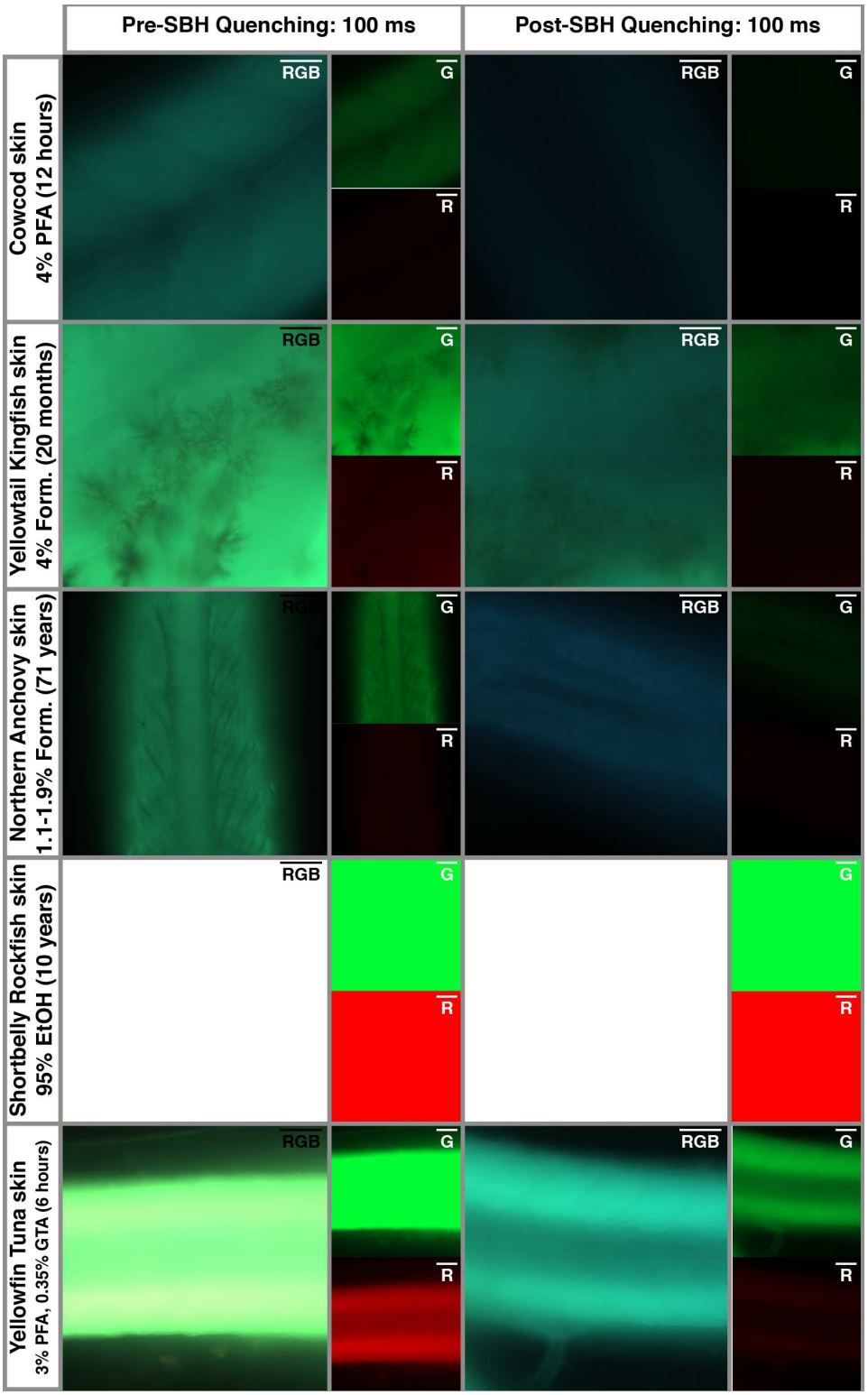

Supplemental Figure 2: Whole-mount epifluorescence images of various archival fish skin before and after sodium borohydride (SBH) quenching. PFA=paraformaldehyde, GTA=glutaraldehyde, EtOH=ethanol. Scale bar=20 μm.